Neuro-Oncology

Neuro-Oncology 16(2), 228–240, 2014
doi:10.1093/neuonc/not215
Advance Access date 4 December 2013

High-throughput microRNA profiling of pediatric high-grade gliomas

Evelina Miele, Francesca Romana Buttarelli, Antonella Arcella, Federica Begalli, Neha Garg, Marianna Silvano, Agnese Po, Caterina Baldi, Giuseppe Carissimo, Manila Antonelli, Gian Paolo Spinelli, Carlo Capalbo, Vittoria Donofrio, Isabella Morra, Paolo Nozza, Alberto Gulino, Felice Giangaspero, and Elisabetta Ferretti

Departments of Experimental and Molecular Medicine, Sapienza University, Rome, Italy (E.M., F.B., N.G., M.S., A.P., C.C., A.G., E.F.); Medico-Surgical Sciences and Biotechnologies, Sapienza University, Rome, Italy (GP.S.); Department of Radiological, Oncological-Pathological Science Sapienza University, Rome, Italy (M. A., F. G.); Department of Neurology and Psichiatry Sapienza University of Rome, Italy (F.R.B., C.B., G.C.); Neuromed Institute, Pozzilli, Italy (A. A.); Pausilipon Hospital, Naples, Italy (V. D.), Regina Margherita Hospital, Torino, Italy (I. M.); Gaslini Pediatric Hospital, Genova, Italy (P. N.); Center for Life NanoScience@Sapienza, Istituto Italiano di Tecnologia, Rome, Italy (E.M., A.G.).

Corresponding author: Elisabetta Ferretti, MD, PhD, Department of Experimental Medicine, Sapienza University, Rome, Italy. Viale Regina Elena, 291 - 00161 Rome, Italy (elisabetta.ferretti@uniroma1.it).

Background. High-grade gliomas (HGGs) account for 15% of all pediatric brain tumors and are a leading cause of cancer-related mortality and morbidity. Pediatric HGGs (pHGGs) are histologically indistinguishable from their counterpart in adulthood. However, recent investigations indicate that differences occur at the molecular level, thus suggesting that the molecular path to gliomagenesis in childhood is distinct from that of adults. MicroRNAs (miRNAs) have been identified as key molecules in gene expression regulation, both in development and in cancer. miRNAs have been investigated in adult high-grade gliomas (aHGGs), but scant information is available for pHGGs.

Methods. We explored the differences in microRNAs between pHGG and aHGG, in both fresh-frozen and paraffin-embedded tissue, by high-throughput miRNA profiling. We also evaluated the biological effects of miR-17-92 cluster silencing on a pHGG cell line.

Results. Comparison of miRNA expression patterns in formalin versus frozen specimens resulted in high correlation between both types of samples. The analysis of miRNA profiling revealed a specific microRNA pattern in pHGG with an overexpression and a proliferative role of the miR-17-92 cluster. Moreover, we highlighted a possible quenching function of miR-17-92 cluster on its target gene PTEN, together with an activation of tumorigenic signaling such as sonic hedgehog in pHGG.

Conclusions. Our results suggest that microRNA profiling represents a tool to distinguishing pediatric from adult HGG and that miR-17-92 cluster sustains pHGG.

Keywords: cancer, expression profiling, microRNA, pediatric gliomas.

Pediatric high-grade gliomas (pHGGs) represent an aggressive brain malignancy that originates from glial progenitors.[1,2] pHGGs are less frequent than adult high-grade gliomas (aHGGs);[3,4] nevertheless, they account for 15% of all pediatric brain tumors and show, for the most part, a similarly ominous clinical outcome with high mortality and morbidity.[2] Recent studies based on high-resolution analysis of copy number and gene expression signatures demonstrated that pediatric and adult HGGs represent a related spectrum of disease distinguished by differences in the frequency of copy number changes, specific gene expression signatures, and IDH1 hotspot mutations only in aHGG.[5–7] In pHGG, several genes within the p53, PI3K/RTK, and RB pathways are targeted by focal gain or loss, but other alterations were found only at low frequency except for PDGFRA and CDKN2A.[8,9] Moreover, a recent study based on exome sequencing revealed somatic mutations in the H3.3-ATRX-DAXX chromatin remodeling pathway, which is highly specific to pediatric glioblastoma (pGBM).[10]

Despite this enormous improvement in understanding the molecular basis of gliomagenesis, the current knowledge is still insufficient to improve disease management: conventional treatments universally fail, and thus there is a crucial need to identify relevant targets for designing new therapeutic agents.

In recent years, several studies have identified a class of small cellular RNAs, termed microRNAs (miRNAs), that act either as oncogenes or tumor suppressors,[11,12] and expression-profiling analyses have revealed characteristic miRNA signatures in a number of human cancers.[13,14] Therefore, miRNAs are promising reliable biomarkers of neurological disorders due to their stability (compared with mRNA) because they are less susceptible to chemical modification and RNAse degradation. Their expression analysis has emerged as a

Received 23 February 2013; accepted 18 October 2013

powerful tool to identifying candidate molecules that play an important role in a large number of malignancies.[15] As a matter of fact, a number of miRNAs contribute to brain development,[16,17] and their expression patterns have been described in different brain cancers. Studies on adult glioblastoma (aGBM) have reported either upregulated (miR-21, miR-10b, miR-221/222, miR-26a, miR-335, miR-451 and miR-486) or downregulated (miR-7, miR-106a, miR-124, miR-128, miR-129, miR-137, miR-139, miR-181a, miR-181b, miR-218, miR-323 and miR-328) miRNAs.[15,18–29] Moreover, miR-17 deregulation, a member of miR-17-92 cluster, has been reported in adult gliomas.[30–33]

Regarding pediatric brain tumors, a few studies conducted in medulloblastoma,[34–36] ependymoma,[37] and low-grade astrocytoma[38] have reported a number of deregulated miRNAs. Recently, Birks et al analyzed 24 pediatric CNS tumors, including 4 pHGGs, and found deregulation of miR-129, miR-142-5p, and miR-25.[39]

In our study, we compared the miRNA expression profile of pHGG, aHGG, and normal brain tissues. First, we analyzed the correlation of miRNA expression profiles using fresh-frozen (FF) and formalin-fixed paraffin-embedded (FFPE) tissues from aHGG. Regression analysis showed a high correlation between both types of samples, suggesting that FFPE could be used equivalently to FF specimens for reliable miRNA analysis. Then, we proceeded to analyze miRNA expression profiles pooling FF and FFPE samples for aHGG and pHGG. We also evaluated the expression levels of a series of genes including MDM2, VEGF, REST, Sonic Hedgehog signaling components, and HGG prognostic markers such as epidermal growth factor receptor (EGFR) and platelet-derived growth factor receptors (PDGFR). Finally, among deregulated miRNAs, we validated the miR-17-92 cluster as an important cue for maintaining proliferation and regulating tumorigenesis in pHGG.

Materials and Methods

Patients and Samples

Tumor samples were collected retrospectively from a bio bank instituted with the contribution of Sapienza University of Rome, Neuromed Institute in Pozzilli-Isernia, Pausilipon Hospital in Naples, Regina Margherita Hospital in Turin, and Gaslini Hospital in Genoa. Both FFPE and FF specimens of high-grade glioma (HGG) were obtained from pediatric and adult patients between 2005 and 2010. The samples were collected during surgical treatment with the approval of each hospital's institutional review board, as previously described.[40] We initially collected 21 adult tumor and 9 pediatric tumor FFPE blocks and profiled miRNAs for all of them. Among these, 17 adult samples and 4 pediatric samples passed the stringent criteria based on RNA quality, quantity, and aHGG internal controls of the TLDA miRNA arrays. Thus 12 pHGG (8 FF + 4 FFPE) samples and 23 aHGG (6 FF + 17 FFPE) samples were available for miRNA profiling, while only FF samples were used for gene expression analysis. Clinical and pathologic features such as age, tumor localization, and WHO grade were also collected and summarized in Table 1. Eight normal brain tissues (3 + a pool of 5) were purchased from Ambion-LifeTechnology (Human Brain Total RNA-AM7962) and from AMS Biotechnology (Europe) (UK) (R1234035-50 Total RNA - Human Adult Normal Tissue-Brain; R1234035-P Total RNA - Human Adult Normal Tissue 5 Donor Pool-Brain; R1234042-10 Total RNA - Human Adult Normal Tissue-Brain: Cerebral Cortex.)

Histology

Paraffin-embedded 3-μm-thick sections from pHGG and aHGG tissues were cut and stained with hematoxylin and eosin for histology. Histology was reviewed by 2 neuropathologists (F.G. and M.A.), and diagnoses were centralized to minimize interobserver variability.

RNA Extraction

Total RNA was extracted by Trizol reagent (Invitrogen) for FF samples, as described earlier,[41] or by miRNeasy kit (Qiagen) for FFPE samples, from 5 to 20 10 mm-thick tissue sections according to the manufacturer's instructions. Total RNA quantity and quality were evaluated using a spectrophotometer (Nanodrop ND-1000, Thermo Scientific).

Quantification and Confirmation of miRNA Expression

miRNA profiling was performed using quantitative RT-PCR with Taqman low density array (TLDA) microfluidic cards (Human miR v3.0, Applied Biosystems). Each TLDA card set contained MGB-labeled probes specific to 754 mature miRNAs and endogenous small nucleolar RNA controls for data normalization and relative quantification. Reverse transcriptase (RT) reactions were performed according to the manufacturer's instructions. Each RT reaction contained purified total RNA and reagents from the Applied Biosystems microRNA Reverse Transcription Kit. Reactions were run in a 384-well TLDA block at 94.5°C for 10 minutes, followed by 40 cycles at 97°C for 30 seconds and 59.7°C for 1 minute. Individual miRNA expression analysis for miR-17-92 family was performed in triplicate in 96-well plates using the TaqMan Individual miRNA assays (Applied Biosystems) according to the manufacturer's instructions. miRNA expression using Taqman probes was performed as described earlier[35] using the following miRNAs: miR-17-5p (Code:002308), miR-18a-5p (Code:002422), miR-19-3p (Code:000395), miR-19b-3p (Code:000396), miR-20a-5p (Code:000580), miR-20b-5p (Code:001014), miR-92a-3p (Code:000430).

Statistical and Graphical Analysis

For all miRNA quantification experiments, cycle threshold (Ct) values >36 were excluded. Values were normalized against the expression levels of RNU6B and RNU48, and delta Ct values were calculated using Real-Time StatMiner software (Integromics TM). The same software was used to generate unsupervised hierarchical clustering based on support tree average linkage with Eucledian correlations. The Wilcoxon signed rank test was performed using StatMiner software (Integromics, TM) to generate delta-delta Ct values for each comparison. *P* values were adjusted using the FDR Benjamini-Hochberg method, and significance was attributed with FDR < 0.05 for all analyses. Supervised hierarchical clustering of differentially expressed miRNAs in pHGG versus aHGG were generated by SpotFire software according to delta Ct values. The clustering and tree were based on Euclidean correlation, complete linkage, and unidimensional scaling using SpotFire software (TIBCO Software, Inc. CA, USA).[34] For gene expression analysis, statistics were performed using StatView 4.1 software (Abacus Concepts). The Mann–Whitney U test for unpaired data was used to analyze differences in gene expression of each gene between pHGG and aHGG. Statistical analysis of biological experimental triplicates was performed using StatView 4.1 software. Mann–Whitney U test for nonparametric values was applied to analyze statistical differences. The results are expressed as mean ± SD from an appropriate number of experiments as indicated in the Figure legends.

miRNA in Situ Distribution

In situ hybridization miRCURY LNA™ miRNA detection (FFPE), optimization kit, and hsa-miR-17, hsa-miR-19a, hsa-miR-92a, detection probes (3′-5′amino-labeled DIG) were purchased from Exiqon. Nuclei were counterstained with Hoechst. The experiment was performed as suggested by the manufacturer using at least 3 pHGG and 3 aHGG samples.

Table 1. Clinicopathologic characteristics of high-grade glioma samples

Sample	Age at diagnosis	Localization	Tissue	Histology	WHO Grade	microRNA	Gene Expression
Pediatric							
1	12	Frontal lobe	Frozen	AA	III	Yes	Yes
2	3	Encephalon, NOS	Frozen	GBM	IV	Yes	Yes
3	17	Temporal lobe	Frozen	GBM	IV	Yes	Yes
4	17	Encephalon, NOS	Frozen	GBM	IV	Yes	Yes
5	13	Encephalon, NOS	Frozen	GBM	IV	Yes	Yes
6	11	Frontal lobe	Frozen	AA	III	Yes	Yes
7	6	Temporal lobe	Frozen	GBM	IV	Yes	Yes
8	5	Encephalon, NOS	Frozen	AA	III	Yes	Yes
9	6	Right frontal lobe	FFPE	GBM	IV	Yes	No
10	11	Mesencephalon	FFPE	GBM	IV	Yes	No
11	7	Temporal lobe	FFPE	AA	IV	Yes	No
12	6	Frontal lobe	FFPE	GBM	IV	Yes	No
Adult							
1	71	Encephalon, NOS	Frozen	GBM	IV	Yes	Yes
2	58	Encephalon, NOS	Frozen	GBM	IV	Yes	Yes
3	61	Encephalon, NOS	Frozen	GBM	IV	Yes	Yes
4	59	Encephalon, NOS	Frozen	GBM	IV	Yes	Yes
5	66	Frontal lobe	Frozen	GBM	IV	Yes	Yes
6	37	Frontal lobe	Frozen	GBM	IV	Yes	Yes
7	55	Frontal lobe	FFPE	GBM	IV	Yes	No
8	48	Left cerebral hemisphere	FFPE	GBM	IV	Yes	No
9	44	Left frontal lobe	FFPE	GBM	IV	Yes	No
10	41	Frontal lobe	FFPE	GBM	IV	Yes	No
11	40	Right frontal lobe	FFPE	GBM	IV	Yes	No
12	34	Right frontal lobe	FFPE	GBM	IV	Yes	No
13	49	Right frontal lobe	FFPE	GBM	IV	Yes	No
14	48	Left frontal lobe	FFPE	GBM	IV	Yes	No
15	49	Right frontal lobe	FFPE	GBM	IV	Yes	No
16	58	Left temporal lobe	FFPE	GBM	IV	Yes	No
17	77	Right temporal lobe	FFPE	AA	III	Yes	No
18	33	Encephalon, NOS	FFPE	AA	III	Yes	No
19	57	Encephalon, NOS	FFPE	AA	III	Yes	No
20	61	Encephalon, NOS	FFPE	AA	III	Yes	No
21	79	Encephalon, NOS	FFPE	AA	III	Yes	No
22	56	Encephalon, NOS	FFPE	GBM	IV	Yes	No
23	18	Frontal lobe	FFPE	GBM	IV	Yes	No

Abbreviations: AA, anaplastic astrocytoma; FFPE, formalin-fixed paraffin-embedded; GBM, glioblastoma multiforme; NOS, not otherwise specified.

Gene Expression Analysis

1 μg of RNA was reverse-transcribed using the High Capacity cDNA Reverse Transcription Kit (Ambion/Life Technologies). Gene expression analysis on all FF samples was performed with ABI Prism 7900 HT sequence detection system (Applied Biosystems/Life Technologies) using TaqMan assays according to the manufacturer's instructions (Biosystems/LifeTechnologies). Each amplification reaction was performed in triplicate, and the average of the 3 threshold cycles was used to calculate the amount of transcripts in the sample (SDS software, Applied Biosystems). mRNA quantification was expressed, in arbitrary units, as the ratio of the sample quantity to the calibrator or to the mean values of control samples. All values were normalized to the following 4 endogenous controls: GAPDH, ß-ACTIN, ß2-MICROGLOBULIN, and HPRT.

Cell Lines and Treatment

KNS42 (pHGG cell line) was obtained from the Health Science Research Resources Bank of the Japan Health Sciences Foundation and grown in DMEM/F12 medium + 10% FCS at 5% CO_2, as previously described.[42,43] U87MG (adult glioma cell line) was purchased from ATCC and was cultured in minimal essential medium + 10% FCS.

Silencing of miRNA was performed using LNA oligonucleotides (Exiqon) against each miRNA of interest, that is, scrambled LNA-miR-Negative control A (code: 199020-08), LNA-miR-17 (code: 426848-00), LNA-miR-18a (code: 428250-08), LNA-miR-19a (code: 426986-08), LNA-miR-19b (code: 426922-08), LNA-miR-20a (code: 411929-08), LNA-miR-92a (code: 411374-04). Single LNA or a pool of LNA at a final concentration of 50 nM was transfected into cells with Hiperfect reagent (Qiagen).

Cell Proliferation and Colony Assays

Cell proliferation of KNS42 and U87MG, after treatment with either scrambled LNA miR control or with a pool of LNA-miR-17-92 cluster, was evaluated by BrdU incorporation (24 h pulse). Cells were fixed with 4% paraformaldehyde, permeabilized with 0.1% Triton X-100, and BrdU detection (Roche) was performed according to the manufacturer's instructions. Nuclei were counterstained with Hoechst reagent. At least 300 nuclei were counted in triplicate, and the number of BrdU-positive nuclei was recorded. For colony formation assays, 120 LNA-transfected KNS42 and 100 LNA-transfected U87MG cells were plated in 10 cm diameter dishes and after-cell colonies were counted after 2 weeks following staining in 20% methanol and crystal violet. KNS42 cells were cultured in self-conditioned medium for 3–4 weeks as described earlier.[43]

Western Blot Assay

Cells were lysed in Tris–HCl pH 7.6, 50 mM, deoxycholic acid sodium salt 0.5%, NaCl 140 mM, NP40 1%, EDTA 5 mM, NaF 100 mM, Na pyrophosphate 2 mM, and protease inhibitors. Lysates were separated on 8% acrylamide gel and immunoblotted using standard procedures. Rabbit anti-PTEN (Cell Signaling), mouse anti-RB1 (*BD* BioSciences), mouse anti-GAPDH (AbCam), and HRP-conjugated secondary antisera (Santa Cruz Biotechnology) were used, followed by enhanced chemiluminescence (ECL). Densitometry calculations for Western blot were calculated using Image-J software (rsb.info.nih.gov), verifying for nonsaturation and subtracting background. Values are expressed as the integrals of each band normalized to weakest band.

Results

Characteristics of Patients and Samples

We collected and included in the study 12 pHGG (8 FF + 4 FFPE) samples and 23 aHGG (6 FF + 17 FFPE) samples. The clinical and pathological features of the specimens used in this study are shown in Table 1 and in Supplementary Fig. S1. Among pediatric samples, 3 were grade III WHO, while 9 (5 FF + 4 FFPE) were grade IV. Adult specimens consisted of 5 samples of grade III and 18 samples (6 FF + 12 FFPE) of grade IV. At the time of data censoring, the median age of our pediatric patient cohort was 9 years, and the average was 9.5 years (range 3–17 years); the median age of the adult patient cohort was 55 years, and the average was 52 years (range 18–79 years). Tumors were all primary HGG, and all were localized in the supratentorial region.

MicroRNA Expression Profiling of Pediatric and Adult High-grade Glioma Samples

To evaluate the effectiveness of FF and FFPE tissues for the measurement of miRNA levels, we profiled the expression levels of 754 miRNAs in all aHGG samples. Our results showed a significant correlation and equivalence in miRNA values between FFPE and FF specimens ($r = 0.82$; $P < .001$) (Fig. 1A), confirming previous report[37,44] and allowing us to pool all samples for a wider high-throughput miRNA-profiling analysis.

Of 754 analyzed miRNAs, 436 were expressed (58%) in HGG. Unsupervised hierarchical clustering of miRNA expression levels revealed that pHGG miRNA profiles clustered separately from aHGG and normal brain tissues (controls), indicating that a number of deregulated miRNAs characterized these tumors (Fig. 1B). The analysis shows that the HGG miRNA pattern can be grouped into 2 main clusters, one composed of only aHGG (left side Fig. 1B) and the other composed of aHGG and pHGG (right side Fig. 1B); there was a much wider internal diversity in the latter with respect to the former. This aHGG/pHGG group was further separated into 2 consistent subgroups, one composed of aHGG, the other by pHGG (Fig. 1B). The pattern of miRNA control samples clustered separately from both aHGG and pHGG. Among the 436 expressed miRNAs, 152 (35%) were differentially expressed between pHGG and controls, as shown in the heat map of supervised hierarchical clustering in Fig. 2A and in Supplementary Table S1 ($P < .02$, FDR < 0.05). Two hundred twenty eight miRNAs (52%) were differentially expressed between pHGG and aHGG, as shown in the heat map of supervised hierarchical clustering in Fig. 2B and in Supplementary Table S2 ($P < .02$, FDR < 0.05). Differentially expressed miRNAs between aHGG versus controls (209 of 436 expressed, 47%) are reported in Supplementary Table S3.

Further analysis of the differentially expressed miRNA between pHGG versus aHGG showed that deregulated miRNAs belonged to a number of genomic clusters as indicated in Table 2. These data suggested a possible common regulation (increased/reduced transcription or genetic amplification/deletion) of specific genomic region coding for differentially expressed miRNAs. Several miRNAs upregulated in pHGG were already known to be "onco-related" (ie, cluster miR-17-92, cluster miR-106b-25 and miR-21), suggesting their potential role in the pathogenesis of these tumors (Supplementary Fig. S2).

Gene Expression Features of pHGG and aHGG

All frozen samples ($n = 14$ HGG; $n = 8$ controls) were also evaluated for their gene expression features. The heat map of all genes evaluated is shown in Fig. 3A. Genes differentially expressed between pHGG versus controls/aHGG or aHGG versus controls are reported in Fig. 3B and in Supplementary Table S4. As a control of this gene expression analysis, we also evaluated genes already known to be markers for HGG such as EGFR for aHGG and PDGFRA and PDGFRB for pHGG.[45,46]

Interestingly, higher levels of GLI1, CCND1, BMP2, and SFRP1 suggested a deregulation of the Sonic Hedgehog pathway in pHGG. Conversely, VEGFA, REST, and MDM2 were more expressed in aHGG.

miR-17-92 Cluster Controls pHGG Proliferation and Tumorigenic Signaling

Gene expression findings, together with miRNA screening results, drove us to further investigate the role of miR-17-92 cluster in pHGG. As already known, the miR-17-92 cluster (also called Oncomir-1) is one of the first miRNA clusters with a validated oncogenic role. Its overexpression has been found in medulloblastoma and neuroblastoma as well as hematopoietic, breast, colon, gastric, and lung cancers.[47–51] Published data have shown that miR-17-92 cluster controls cell proliferation in response to the activation of Sonic Hedgehog pathway in brain development and cancer.[47,52–54] Recently, we have identified a direct regulation of miR-17-92 cluster by Sonic Hedgehog pathway.[55]

Mir-17-92 cluster consists of 6 miRNAs that can be subgrouped into 4 families based on their "seed" sequence (the determinant region of target specificity). These include miR-17 family (miR-17, miR-20a), miR-18 family (miR-18a), miR-19 family (miR-19a,

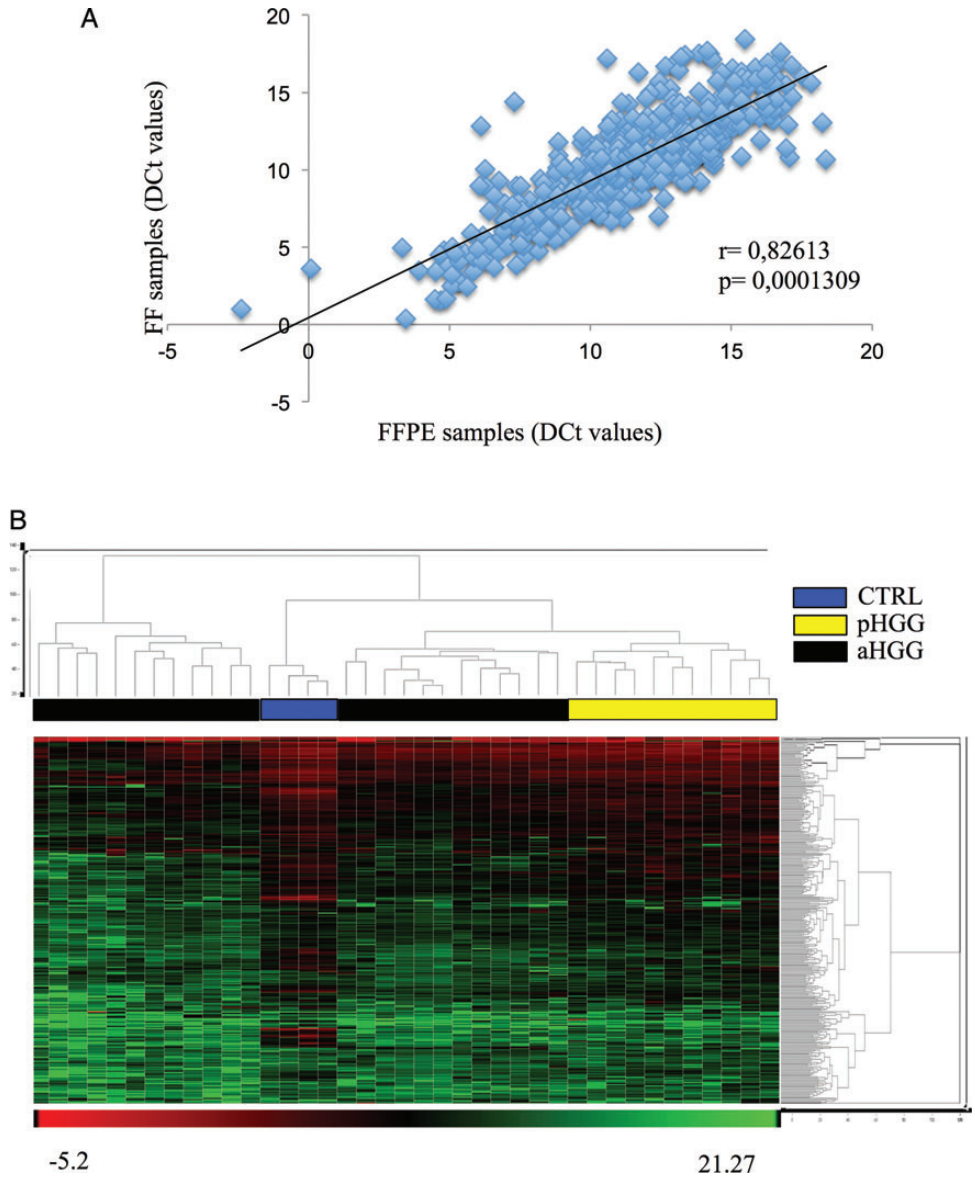

Fig. 1. miRNA profiles of pHGG and aHGG. (A) Regression analysis of adult samples formalin-fixed paraffin-embedded (FFPE) versus fresh-frozen (FF). Scatter plot showing Spearman correlation between FF and FFPE groups. (B) Unsupervised hierarchical clustering of pediatric HGG (pHGG), adult HGG (aHGG) and normal brain tissues (CTRL). The clustering and tree are based on Euclidian correlations and were generated by Integromics software according to delta Ct values. The supporting tree on the top shows the separation of normal brain tissues from tumor samples and a part of aHGG samples clustering together with pHGG. The tree on the right shows miRNA clusters. Black: aHGG, Yellow: pHGG, Blue: CTRL.

miR-19b), and miR-92 family (miR-92a).[31] We first validated array data by RT-qPCR analyses of each miRNA in all tumors, confirming the overexpression of miR-17-92 cluster in pHGG (Fig. 4A). Next, we analyzed the distribution of the miR-17-92 cluster in pHGG and aHGG by in situ hybridization analysis. Results showed positive staining in both tumors, which was more intense in pHGG. Results on miR-19a and miR-17 are reported in Fig. 4B.

To gain insight into the biological role of the miR-17-92 cluster, we studied the effects of its silencing in a pediatric glioma cell line (KNS42) (Fig. 5A). We observed a reduction of cell proliferation after individual and miRNA whole-cluster silencing using LNA-modified antagomirs. The abrogation of the whole cluster (LNA-mix) significantly affected the proliferation rate ($P < .05$) (Fig. 5B). The miRNA effects on cell proliferation were also confirmed by cell colony formation assays. Indeed, silencing of all components of miR-17-92 significantly reduced the number of KNS42 cell colonies (Fig. 5C and D). The same experiments were performer in adult glioma cell line U87MG, where miR-17-92 cluster silencing did not significantly affect cell colony number (Supplementary Fig. S3).

Finally, in order to further shed light on the role of miR-17-92 cluster in pHGG gliomagenesis, we searched for putative and validated targets of each family using the prediction algorithms of TargetScan, miRDB, PicTar, and MiRtarBase (Table 3). We investigated the expression levels of 25 of them in pHGG. Results are shown in

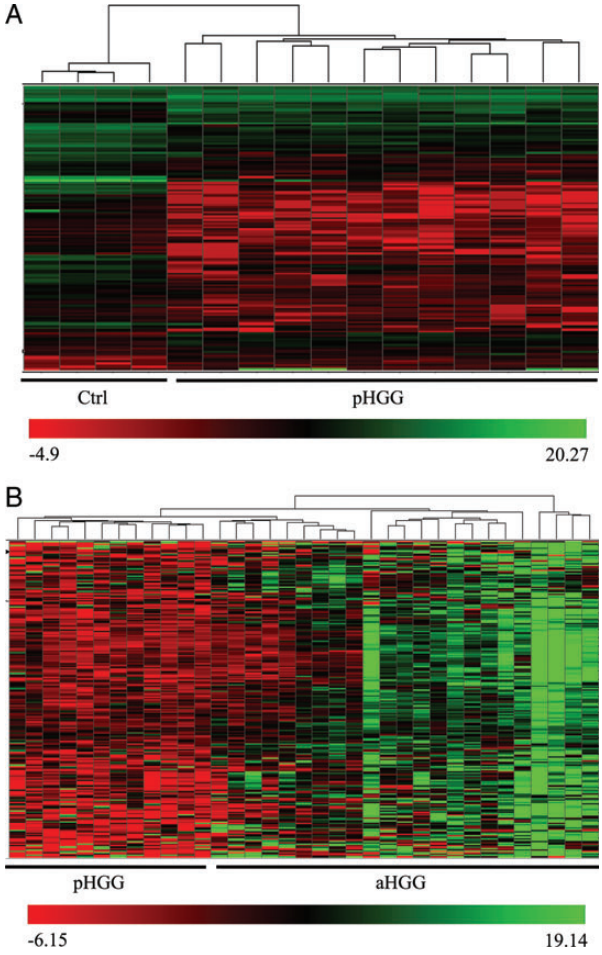

Fig. 2. Supervised hierarchical clustering of differentially expressed miRNAs. (A) Supervised hierarchical clustering with 152 differentially expressed miRNAs between pHGG and controls ($P < .02$; FDR < 0.05). (B) Supervised hierarchical clustering with 228 miRNAs identified as differentially expressed in pHGG when compared with aHGG ($P < .02$; FDR < 0.05). The clustering and tree are based on Euclidean correlation and were generated according to delta Ct values.

Table 2. Clusters of microRNA upregulated in pediatric high-grade glioma versus adult high-grade glioma and controls

Chromosome	cluster of microRNA
1	miR-29b-2, miR-29c
	miR-30c-1, miR-30e
3	**miR-15b**, miR-16-2
	miR-191, miR-425
	miR-193b, miR-365a
7	**miR-106b miR-93, miR-25**
8	miR-30d, miR-30b
9	let-7a-1, let-7d, let-7f-1
	miR-23b, miR-27b, miR-24-1
11	let-7a-2, **miR-100**
13	**miR-15a**, miR-16
	miR-17, miR-18a, miR-19a, miR-20a, miR-19b, miR-92°
14	miR-337, miR-665, miR-431, miR-433, miR-127, miR-432, miR-136*
	miR-665, miR-431, miR-433, miR-127, miR-432, miR-136*
	miR-543, miR-495, miR-376c, miR-376a, miR-654, miR-376a-1, miR-487b, miR-539, miR-889, miR-665
	miR-411, miR-380, miR-323a, miR-758, miR-543
	miR-323b, miR-496, miR-541, miR-409, miR- 410
	miR-487b, miR-539, miR-889, miR-655, miR-487a, miR-134 miR-323b, miR-496, miR-541
	miR-543, miR-495, miR-376c, miR-376a-2, miR-654, miR-376a-1, miR- 487b, miR-539, miR-889, miR- 655
17	miR-132, miR-212
	miR-193b, miR-365°
	miR-195, miR-497
19	let-7e, miR-99b, miR-125°
	miR-23a, **miR-27a**, miR-24-2
21	let-7c, miR-99a
22	let-7a-3, let-7b,
X	let-7f-2, miR-98
	miR-106a, miR-18b, miR-20b, miR-19b-2, miR-92a-2
	miR-532, miR-362, mir-501, miR-660, miR-502
	miR-545, miR-374a

Table reports all microRNAs significantly upregulated in pHGG versus aHGG ($P < .05$); The microRNAs depicted in bold-face type represent significant upregulation versus normal brain tissues (Ctrl).

Fig. 6A, where genes are grouped by each miR family. Among the target molecules downregulated in pHGG, we found PTEN and RB1. Silencing of the miR-17-92 cluster in KNS42 cell line resulted in PTEN and RB1 upregulation, which supported a possible role of this cluster in the control of oncosuppressor genes in pHGG (Fig. 6B and C).

Discussion

The accumulation of large datasets on aHGG has revealed key biological differences between adult and pediatric tumors.[5] Furthermore, subclassifications within the childhood age group can be made depending on age at diagnosis and tumor site.[56] However, challenges remain on how to reconcile clinical data from adult patients to tailor novel treatment strategies specifically for pediatric patients. pHGG tumors have escaped the extensive investigation that has been undertaken for adults because of their rarity, the widespread sampling among many neurosurgical units, and the lack of a collaborative research network.

In the last years, miRNA expression profiles were reported in different pediatric brain tumor types.[34–39] The present study is the first that specifically characterizes miRNA profiles of pHGG. One of the major limiting factors to studying the molecular alterations in childhood HGG, particularly by microarray and transcript analysis, is the need for FF material, which allows the extraction of high-quality nucleic acids. On the other hand, FFPE tissue specimens, even they do not permit extraction of good-quality nucleic acids, are correlated with precious clinical and follow-up data. We took advantage of the opportunity to gather data from a wider cohort of pHGG, driven by the equivalence in miRNA profile results from FFPE and FF tumor samples, as already reported.[37,44] Recently,

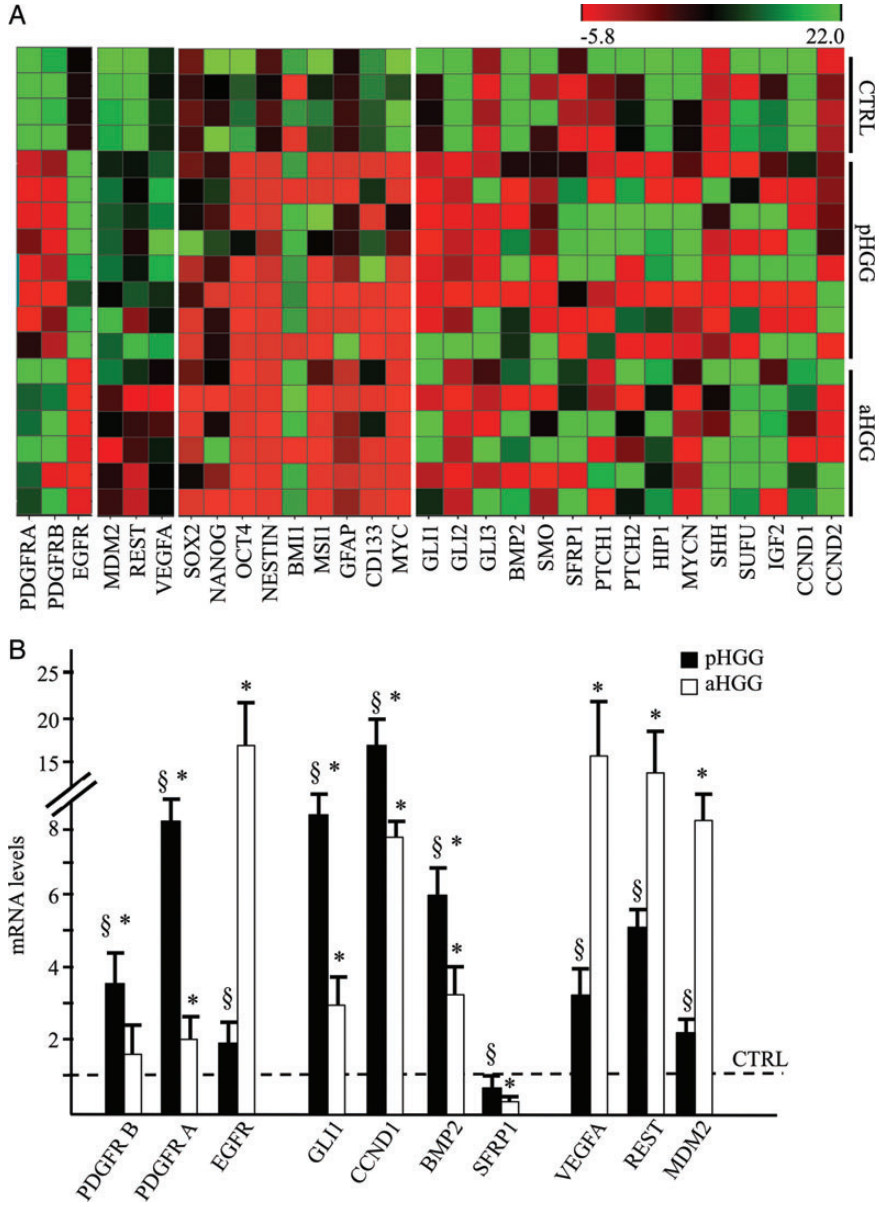

Fig. 3. Differentially expressed genes in pHGG versus normal brain tissues and aHGG. (A) Heat map of expression levels of the indicated genes in pHGG, aHGG, and normal brain tissues as control (CTRL). A green-red color scale depicts normalized delta Ct values. (B) Histogram shows statistically differentially expressed genes in pHGG and aHGG with respect to controls (dashed lines) (*$P < .05$); Differentially expressed genes in pHGG versus aHGG are also reported (§ $P < .05$ vs aHGG).

Birks et al analyzed miRNA profiles in 24 pediatric CNS tumors including 4 HGG WHO grade IV. Our study includes a wider series of pHGGs, confirming a deregulation of miRNA-129, miR-142-5p, and miR-25 that suggests their general role in all pediatric brain tumorigeneses.[39] By extending these findings, we were able to describe specifically deregulated miRNAs in pHGG that highlighted the upregulation of miR-17-92 cluster. The differential expression of the miR-17-92 cluster between pHGG and aHGG could be a diagnostic tool: we speculate the possibility of discriminating different disease in ages that fall inside the boundary of the 2 categories such as adolescence and young adulthood. This is an important issue because pHGGs are histologically indistinguishable from their counterparts in adulthood. However, recent investigations indicate that differences occur at the molecular level and therefore the molecular programs to gliomagenesis in childhood are distinct from those encountered in adults.

The first expression-profiling study identified 2 subgroups of pGBM that were distinguished by the differential expression of a gene signature indicative of activated PI3K and Ras signaling.[6,57] A subsequent larger series by Paugh et al[5] further defined the differences and similarities between childhood and adult HGG. In that study, 3 subgroups of pHGG seem to overlap, albeit superficially, with the aHGG expression subclasses proposed by Phillips et al.[9,56] The Phillips' signatures were defined by proneural,

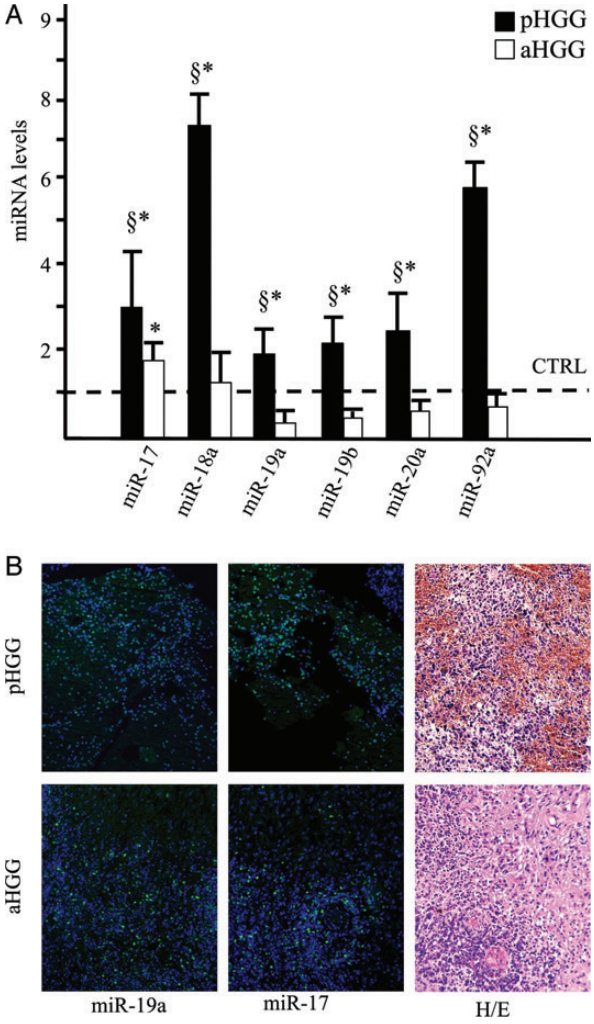

Fig. 4. miRNA-17–92 cluster in pHGG and aHGG. (A) qRT-PCR analysis of each member of the miRNA-17-92 cluster in pHGG and aHGG versus normal brain tissue as control (CTRL, dashed line). Bars represent the mean of 3 independent experiments ± SD. *$P < .05$ pHGG versus control tissues, § $P < .05$ pHGG versus aHGG. (B) Detection and localization of miR-17 and miR-19a (green) by in situ hybridization (ISH), nuclear counterstaining (Hoechst-blue) and hematoxylin and eosin staining (H/E) in pHGG and aHGG samples.

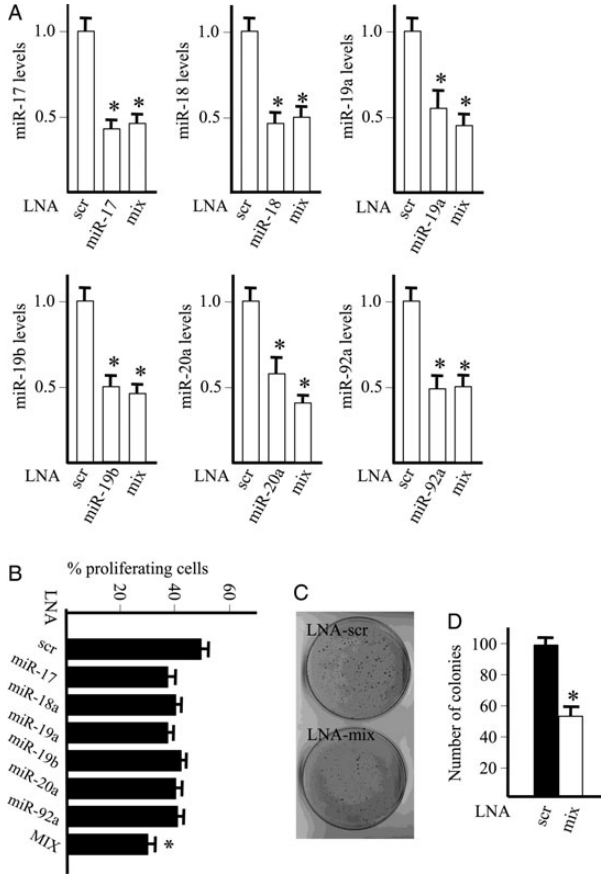

Fig. 5. miR-17-92 cluster controls pHGG. (A) Histograms showing the levels of miR-17-92 cluster members in pediatric glioma cell line KNS42 after LNA-mediated silencing of each miR and the combination of all (LNA-mix), compared with LNA-scramble as control (scr-LNA). Graph error bars indicate standard deviation calculated on at least 3 independent experiments. * $P < .05$ versus Ctrl. (B) Results of the BrdU assay to assess the cell proliferation rate after individual miRNA silencing and after complete cluster silencing (MIX) compared with LNA-scramble as control (scr). (*$P < .05$). (C) Picture samples of cell colony formation assays of pediatric glioma cell line KNS42 after silencing of all components miR-17-92 (LNA-mix) versus LNA-scramble as control (LNA-scr). (D) Counts of colonies formed in C. (The values have been normalized, attributing the score of 100 to the number of colonies grown from control-transfected cells, ctrl) (*$P < .05$).

proliferative, and mesenchymal gene signatures, among which the latter 2 were also identified in the pGBMs studied by Faury et al.[57] Moreover, the study of Paugh et al[5] identified a subset of childhood samples that clustered with adult cases. Thus, similar transcriptional programs clearly underlie subclasses of HGG irrespective of age. The biological distinctiveness of pHGG was conclusively demonstrated in a comprehensive whole-exome gene sequencing study of 48 cases of pGBM.[10] The study revealed that in 44% of tumors, somatic mutations occurred in the histone H3.3–ATRX–DAXX chromatin-remodeling pathway. Critically, these mutations seem to be specific to children and young adults with glioblastoma.[58] Our results are in accordance with the literature data, especially regarding the upregulation of EGFR in aHGG and PDGFRA-B in pHGG.[5,45,46] Indeed, inhibition of PDGFR by imatinib and the combination with other targeted agents, such as inhibition of IGF1R, may be a useful therapeutic strategy in pGBM.[59] The high levels of VEGF in our series of aHGGs confirm that aHGGs are highly vascularized brain tumors[60] and that anti-VEGF treatment is an important therapeutic strategy.[61] We also showed an aberrant maintenance of REST expression in aHGG, as reported earlier with glioblastoma stem cells.[62] Gene amplification of MDM2 has been described as a prognostic marker in glioblastoma and its activation appears to occur late in tumor progression.[63]

Our data show that the Sonic Hedgehog pathway is more expressed in all tumors, both adult and pediatric HGGs respect to normal brain tissues. Previous studies provided evidence for the role of this signaling in adult gliomas.[52,54] Here we report that Sonic Hedgehog pathway upregulation also occurs in pHGG.

Table 3. Target genes of miR-17/92 cluster

miR	Family	Genes	Validated	References	Sources
miR-17	miR-17	TP53INP1	Yes	Lewis BC 2005; Grimson A 2007; Friedman RC 2009; Krek A 2005	targetscan/pictar
		MYCN	Yes		targetscan/pictar
		RBL1	Yes		targetscan/mirtarbase/pictar
		HLF	Yes		targetscan/pictar
		CRK	Yes		targetscan/pictar
		FGF-5	Yes	Garcìa 2011	targetscan
		ACVR1B	No		targetscan
		BCL2L11	Yes	Olive V 2013;	targetscan
		BMPR2	No		targetscan/pictar
		CAPRIN1	No		targetscan/pictar
		CDC25A	No		targetscan
		CDK6	No		targetscan/pictar
		CDKN1A	Yes	He M 2013	targetscan/pictar
		CLYD	Yes	Jin HY 2013	targetscan/pictar
		EGR2	Yes	Pospisil V 2011	targetscan/pictar
		JAK1	Yes	Doebele C 2010	targetscan/pictar
		LUZP1	No		targetscan
		MECP2	No		targetscan
		NR4A3	No		targetscan
		SMAD7	No		targetscan/pictar
		PTEN	Yes	Shan SW 2013	targetscan/pictar
		RB1	Yes	Trompeter HI 2011	targetscan/pictar
miR-18a	miR-18	ATM	Yes	Song L 2011, Friedman RC 2009; Hsu SD 2011	targetscan/mirtarbase
		HLF	Yes	Garcia DM 2011	targetscan
		PDGFRB	Yes	Garcia DM 2011	targetscan
		ABL1	Yes	Garcia DM 2011	targetscan
		KRAS	Yes	Hsu SD 2011	mirtarbase
		NCOA1	Yes	Lewis BC 2005; Grimson A 2007; Friedman RC 2009;	targetscan
		MUM1	No		targetscan
miR-19a	miR-19	MYCN	Yes	Lewis BC 2005; Grimson A 2007; Friedman RC 2009; Krek A 2005	targetscan/pictar
		WNT3	Yes		targetscan/pictar
		BCL3	Yes		targetscan/pictar
		TP53INP1	Yes		targetscan/pictar
		RAF1	Yes		targetscan/pictar
		FGF6	Yes	Friedman 2009	targetscan
		APAF1	No		targetscan
		BMP3	No		targetscan
		CTGF	Yes	Olive V 2013;	targetscan
		MAPK1	No		targetscan
		PPARA	No		targetscan
		RAB8B	No		targetscan
		RASGRP1	No		targetscan
		SDC1	No		targetscan
		CLYD	Yes	Huashan Ye 2012	targetscan/pictar
		PTEN	Yes	Wang F 2013	targetscan/pictar
miR-20	miR-17	CCND1	Yes	Hsu SD 2011	mirtarbase
		MYCN	Yes	Hsu SD 2011; Wang F 2008	mirtarbase/miRDB
		HLF	Yes	Krek A 2005; Wang F 2008	miRDB/pictar
		TP73	Yes	Garcìa 2011	targetscan
		MLL	Yes	Garcìa 2011	targetscan
		PDGFRA	Yes	Lewis BC 2005; Grimson A 2007; Friedman RC 2009; Krek A 2005	targetscan/pictar
		PTEN	Yes	Poliseno L 2010	targetscan/pictar
		RB1	Yes	Trompeter HI 2011	targetscan/pictar

Continued

Table 3. *Continued*

miR	Family	Genes	Validated	References	Sources
miR-19b	miR-19	USP6	Yes	Krek A 2005; Wang 2008	pictar/miRDB
		ERBB4	Yes	Krek A 2005	pictar
		BCL3	Yes	Krek A 2005; Wang 2008	pictar/miRDB
		KRAS2	Yes	Krek A 2005	pictar
		RAF1	Yes	Krek A 2005; Wang 2008	pictar/miRDB
		MYCN	Yes	Hsu SD 2011; Wang 2008	mirtarbase/miRDB
		PTEN	Yes	Wang F 2013	targetscan/pictar
miR-92a	miR-25	MCL1	Yes	Grimson A 2007; Friedman RC 2009;	pictar/targetscan
		BCL2L11	Yes	Krek A 2005; Hsu SD 2011; Wang 2008	pictar/mirtarbase/miRDB
		BCL9	Yes	Krek A 2005	pictar
		BCAT2	Yes	Lewis BC 2005; Grimson A 2007; Friedman RC 2009; Hsu SD 2011	pictar/miRDB/targetscan
		NOTCH1	Yes		targetscan
		RAB23	Yes		targetscan/miRDB
		MEF2D	No		targetscan/miRDB

Source: bioinformatic tools of targetscan, miRDB, pictar, miRtarBase.

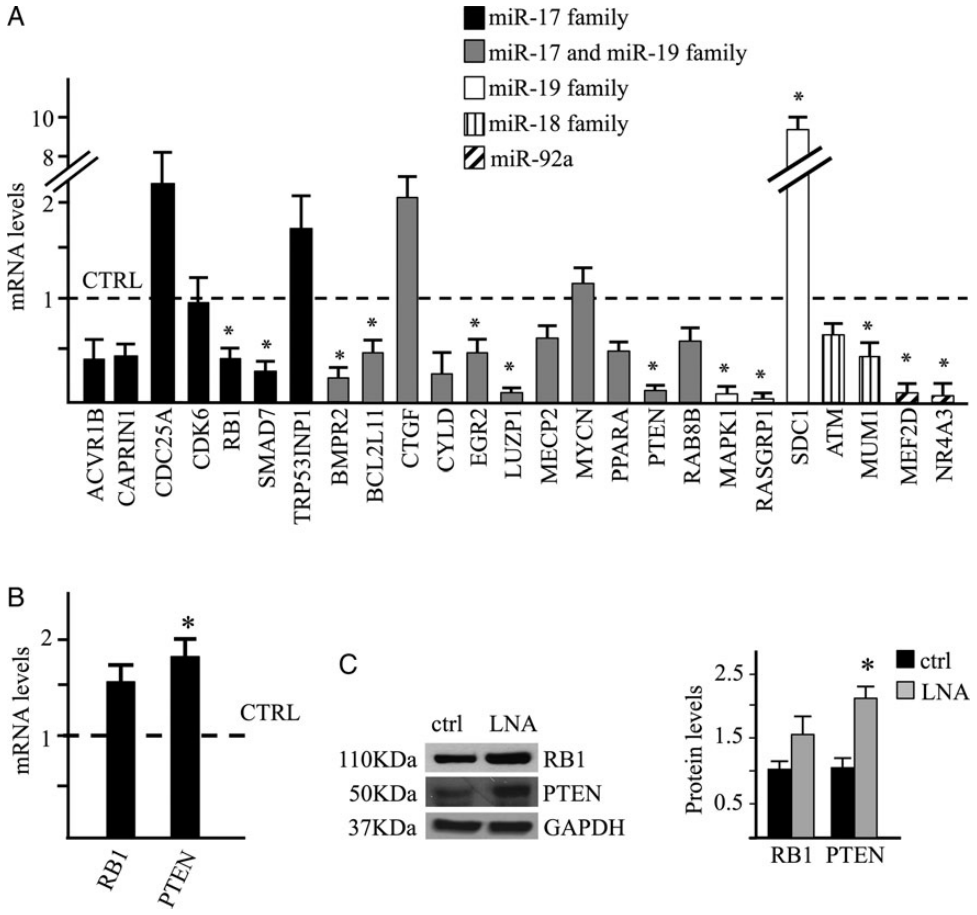

Fig. 6. Target genes of miR-17-92 cluster in pHGG. (A) Histograms showing the mRNA levels of miR-17-92 cluster target genes evaluated by qRT-PCR in pHGG compared with normal brain tissues as controls (CTRL). Different colors of columns have been used to differentiate each miR-family target genes.(* $P < .05$ vs ctrl) (B) mRNA levels of RB1 and PTEN in pHGG cell line SKN-42 after LNA-mediated silencing of miR-17-92 cluster compared with LNA-scramble transfected cells as control (ctrl). (*$P < .05$). (C) Left panel. Western blot assay showing protein levels of RB1 and PTEN, together with GAPDH as loading control, in SKN-42 pHGG cell line transfected with LNA-miR-17-92 cluster or LNA-scramble (ctrl). Right panel. Densitometry of Western blot for RB1 and PTEN protein evaluation after miR-17-92 cluster reported in upper panel. Bars represent the mean of 3 independent experiments ± SD (*$P < .05$ vs ctrl).

These data are not surprising since pHGGs are characterized by high PDGFRs and Hedgehog has already been reported as being connected to PDGF-induced gliomagenesis.[64] Moreover, pHGG could originate from cells with stemness properties sustained by Hedgehog. Indeed, some stemness-related molecules have higher expression levels in pHGG than in aHGG samples (eg, CD133 and MSI1, Fig. 3 and Supplementary Table S4).

Published data have shown that Sonic Hedgehog pathway controls cell proliferation through miR-17-92 cluster in brain development and cancer.[47,52–54] Moreover, in the neuronal stemness context, we have recently identified a direct regulation of miR-17-92 cluster by Sonic Hedgehog pathway.[55] Given this background, we aimed to investigate the role of this cluster in pHGG. miR-17-92 cluster is able to control cell cycle by inhibiting p53[31] and MDM2 blocks p53 in aHGG.[65] Recently, miR-17-92 cluster has been reported as able to replace MDM2, cooperate with E1A, and activate Ras signaling.[66] In our series of pHGG, the high levels of miR-17-92 cluster could sustain similar oncogenic function(s) as MDM2 in aHGG. Moreover, Ernst et al[67] observed decreased levels of miR-17-92 cluster after differentiation of glioblastoma spheroid cultures, sustaining a linkage between of miR-17-92 cluster and stemness features.[55]

We screened miR-17-92 cluster target genes and interestingly found that several of them downregulated in pHGG samples. Moreover, among them, PTEN and RB1 were upregulated after the cluster silencing in pHGG cells. PTEN, a negative regulator of PI3K-RTK pathway, is frequently inactivated by mutations or deletions (LOH chromosome 10) in aHGG. In pHGG, these genetic events are less common, despite under expression of PTEN is however reported.[8,9] Our results suggest that PTEN downregulation in pHGG could result from the overexpression of the miR-17-92 cluster.

RB1 mutations have been reported in pHGG, although in a lower frequency than in aHGG.[8,9] Our data support a possible involvement of miR-17-92 cluster in repressing the tumor suppressor gene RB1 in pHGG. Thus, we speculate that PI3K/RTK and RB pathways are involved in both adult and in pediatric gliomagenesis, although triggered by different events (genetic loss or miRNA control, respectively).

In conclusion, the present study confirms the equivalence in miRNA profile results from FFPE and FF tumor samples, as already reported,[37,44] an issue certain to be of interest for biomarker studies. Furthermore, our results led to highlighting new molecular aspects of pediatric and adult HGG that support their biological differences. Finally, we revealed that the miR-17-92 cluster is upregulated in pHGG, where it controls cell proliferation and targets tumor suppressor genes such as PTEN.

Supplementary Material

Supplementary material is available online at *Neuro-Oncology* (http://neuro-oncology.oxfordjournals.org/).

Funding

This work was supported by Associazione Italiana per la Ricerca sul Cancro (AIRC), by Ministry of University and Research (FIRB and PRIN), by Ministry of Health, by FP7 Healing (contract PITN-GA-2009-238186), by Istituto Italiano di Tecnologia (IIT) and by Fondazione Italiana Neuroblastoma-Progetto Pensiero.

Conflict of interest statement. None declared.

References

1. Louis DN, Ohgaki H, Wiestler OD, et al. The 2007 WHO classification of tumours of the central nervous system. *Acta Neuropathol*. 2007; 114(2):97–109.
2. Kaatsch P, Rickert CH, Kuhl J, Schuz J, Michaelis J. Population-based epidemiologic data on brain tumors in German children. *Cancer*. 2001;92(12):3155–3164.
3. Fangusaro J. Pediatric high grade glioma: a review and update on tumor clinical characteristics and biology. *Front Oncol*. 2012;2:105.
4. Spinelli GP, Miele E, Lo Russo G, et al. Chemotherapy and target therapy in the management of adult high- grade gliomas. *Curr Cancer Drug Targets*. 2012;12(8):1016–1031.
5. Paugh BS, Qu C, Jones C, et al. Integrated molecular genetic profiling of pediatric high-grade gliomas reveals key differences with the adult disease. *J Clin Oncol*. 2010;28(18):3061–3068.
6. Haque T, Faury D, Albrecht S, et al. Gene expression profiling from formalin-fixed paraffin-embedded tumors of pediatric glioblastoma. *Clin Cancer Res*. 2007;13(21):6284–6292.
7. Johnson R, Wright KD, Gilbertson RJ. Molecular profiling of pediatric brain tumors: insight into biology and treatment. *Curr Oncol Rep*. 2009;11(1):68–72.
8. Bax DA, Mackay A, Little SE, et al. A distinct spectrum of copy number aberrations in pediatric high-grade gliomas. *Clin Cancer Res*. 2010; 16(13):3368–3377.
9. Jones C, Perryman L, Hargrave D. Paediatric and adult malignant glioma: close relatives or distant cousins?. *Nat Rev Clin Oncol*. 2012; 9(7):400–413.
10. Schwartzentruber J, Korshunov A, Liu XY, et al. Driver mutations in histone H3.3 and chromatin remodelling genes in paediatric glioblastoma. *Nature*. 2012;482(7384):226–231.
11. Esquela-Kerscher A, Slack FJ. Oncomirs - microRNAs with a role in cancer. *Nat Rev Cancer*. 2006;6(4):259–269.
12. He L, Thomson JM, Hemann MT, et al. A microRNA polycistron as a potential human oncogene. *Nature*. 2005;435(7043):828–833.
13. Calin GA, Croce CM. MicroRNA signatures in human cancers. *Nat Rev Cancer*. 2006;6(11):857–866.
14. Lu J, Getz G, Miska EA, et al. MicroRNA expression profiles classify human cancers. *Nature*. 2005;435(7043):834–838.
15. De Smaele E, Ferretti E, Gulino A. MicroRNAs as biomarkers for CNS cancer and other disorders. *Brain Res*. 2010;1338:100–111.
16. Kosik KS. The neuronal microRNA system. *Nat Rev Neurosci*. 2006;7(12): 911–920.
17. Smirnova L, Grafe A, Seiler A, Schumacher S, Nitsch R, Wulczyn FG. Regulation of miRNA expression during neural cell specification. *Eur J Neurosci*. 2005;21(6):1469–1477.
18. Chan JA, Krichevsky AM, Kosik KS. MicroRNA-21 is an antiapoptotic factor in human glioblastoma cells. *Cancer Res*. 2005;65(14): 6029–6033.
19. Ciafre SA, Galardi S, Mangiola A, et al. Extensive modulation of a set of microRNAs in primary glioblastoma. *Biochem Biophys Res Commun*. 2005;334(4):1351–1358.
20. Corsten MF, Miranda R, Kasmieh R, Krichevsky AM, Weissleder R, Shah K. MicroRNA-21 knockdown disrupts glioma growth in vivo and displays synergistic cytotoxicity with neural precursor cell delivered S-TRAIL in human gliomas. *Cancer Res*. 2007;67(19):8994–9000.

21. Silber J, Lim DA, Petritsch C, et al. miR-124 and miR-137 inhibit proliferation of glioblastoma multiforme cells and induce differentiation of brain tumor stem cells. *BMC Med*. 2008;6:14.
22. Kefas B, Godlewski J, Comeau L, et al. microRNA-7 inhibits the epidermal growth factor receptor and the Akt pathway and is down-regulated in glioblastoma. *Cancer Res*. 2008;68(10): 3566–3572.
23. Conti A, Aguennouz M, La Torre D, et al. miR-21 and 221 upregulation and miR-181b downregulation in human grade II-IV astrocytic tumors. *J Neurooncol*. 2009;93(3):325–332.
24. Shi L, Cheng Z, Zhang J, et al. hsa-mir-181a and hsa-mir-181b function as tumor suppressors in human glioma cells. *Brain Res*. 2008;1236: 185–193.
25. Jiang J, Sun X, Wang W, et al. Tumor microRNA-335 expression is associated with poor prognosis in human glioma. *Med Oncol*. 2012; 29(5):3472–3477.
26. Wu Z, Sun L, Wang H, et al. MiR-328 expression is decreased in high-grade gliomas and is associated with worse survival in primary glioblastoma. *PLoS One*. 2012;7(10):e47270.
27. Hermansen SK, Dahlrot RH, Nielsen BS, Hansen S, Kristensen BW. MiR-21 expression in the tumor cell compartment holds unfavorable prognostic value in gliomas. *J Neurooncol*. 2013;111(1):71–81.
28. Huse JT, Brennan C, Hambardzumyan D, et al. The PTEN-regulating microRNA miR-26a is amplified in high-grade glioma and facilitates gliomagenesis in vivo. *Genes Dev*. 2009;23(11):1327–1337.
29. Yang G, Zhang R, Chen X, et al. MiR-106a inhibits glioma cell growth by targeting E2F1 independent of p53 status. *J Mol Med (Berl)*. 2011; 89(10):1037–1050.
30. Malzkorn B, Wolter M, Liesenberg F, et al. Identification and functional characterization of microRNAs involved in the malignant progression of gliomas. *Brain Pathol*. 2010;20(3):539–550.
31. Olive V, Jiang I, He L. mir-17–92, a cluster of miRNAs in the midst of the cancer network. *Int J Biochem Cell Biol*. 2010;42(8):1348–1354.
32. Tagawa H, Karube K, Tsuzuki S, Ohshima K, Seto M. Synergistic action of the microRNA-17 polycistron and Myc in aggressive cancer development. *Cancer Sci*. 2007;98(9):1482–1490.
33. Lu S, Wang S, Geng S, Ma S, Liang Z, Jiao B. Increased Expression of microRNA-17 Predicts Poor Prognosis in Human Glioma. *J Biomed Biotechnol*. 2012;2012:970761.
34. Ferretti E, De Smaele E, Po A, et al. MicroRNA profiling in human medulloblastoma. *Int J Cancer*. 2009;124(3):568–577.
35. Ferretti E, De Smaele E, Miele E, et al. Concerted microRNA control of Hedgehog signalling in cerebellar neuronal progenitor and tumour cells. *EMBO J*. 2008;27(19):2616–2627.
36. Venkataraman S, Birks DK, Balakrishnan I, et al. MicroRNA 218 acts as a tumor suppressor by targeting multiple cancer phenotype-associated genes in medulloblastoma. *J Biol Chem*. 2013;288(3):1918–1928.
37. Costa FF, Bischof JM, Vanin EF, et al. Identification of microRNAs as potential prognostic markers in ependymoma. *PLoS One*. 2011;6(10): e25114.
38. Ho CY, Bar E, Giannini C, et al. MicroRNA profiling in pediatric pilocytic astrocytoma reveals biologically relevant targets, including PBX3, NFIB, and METAP2. *Neuro Oncol*. 2013;15(1):69–82.
39. Birks DK, Barton VN, Donson AM, Handler MH, Vibhakar R, Foreman NK. Survey of MicroRNA expression in pediatric brain tumors. *Pediatr Blood Cancer*. 2011;56(2):211–216.
40. Ferretti E, Di Marcotullio L, Gessi M, et al. Alternative splicing of the ErbB-4 cytoplasmic domain and its regulation by hedgehog signaling identify distinct medulloblastoma subsets. *Oncogene*. 2006;25(55): 7267–7273.
41. Po A, Ferretti E, Miele E, et al. Hedgehog controls neural stem cells through p53-independent regulation of Nanog. *EMBO J*. 2010;29(15): 2646–2658.
42. Gaspar N, Marshall L, Perryman L, et al. MGMT-independent temozolomide resistance in pediatric glioblastoma cells associated with a PI3-kinase-mediated HOX/stem cell gene signature. *Cancer Res*. 2010;70(22):9243–9252.
43. Takeshita I, Takaki T, Kuramitsu M, et al. Characteristics of an established human glioma cell line, KNS-42. *Neurol Med Chir (Tokyo)*. 1987;27(7):581–587.
44. de Biase D, Visani M, Morandi L, et al. miRNAs expression analysis in paired fresh/frozen and dissected formalin fixed and paraffin embedded glioblastoma using real-time pCR. *PLoS One*. 2012;7(4): e35596.
45. Sung T, Miller DC, Hayes RL, Alonso M, Yee H, Newcomb EW. Preferential inactivation of the p53 tumor suppressor pathway and lack of EGFR amplification distinguish de novo high grade pediatric astrocytomas from de novo adult astrocytomas. *Brain Pathol*. 2000; 10(2):249–259.
46. Puget S, Philippe C, Bax DA, et al. Mesenchymal transition and PDGFRA amplification/mutation are key distinct oncogenic events in pediatric diffuse intrinsic pontine gliomas. *PLoS One*. 2012;7(2): e30313.
47. Northcott PA, Fernandez LA, Hagan JP, et al. The miR-17/92 polycistron is up-regulated in sonic hedgehog-driven medulloblastomas and induced by N-myc in sonic hedgehog-treated cerebellar neural precursors. *Cancer Res*. 2009;69(8):3249–3255.
48. Luo H, Zou J, Dong Z, Zeng Q, Wu D, Liu L. Up-regulated miR-17 promotes cell proliferation, tumour growth and cell cycle progression by targeting the RND3 tumour suppressor gene in colorectal carcinoma. *Biochem J*. 2012;442(2):311–321.
49. Fontana L, Fiori ME, Albini S, et al. Antagomir-17–5p abolishes the growth of therapy-resistant neuroblastoma through p21 and BIM. *PLoS One*. 2008;3(5):e2236.
50. Osada H, Takahashi T. let-7 and miR-17–92: small-sized major players in lung cancer development. *Cancer Sci*. 2011;102(1):9–17.
51. Zhou H, Guo JM, Lou YR, et al. Detection of circulating tumor cells in peripheral blood from patients with gastric cancer using microRNA as a marker. *J Mol Med (Berl)*. 2013;88(7):709–717.
52. Dahmane N, Sanchez P, Gitton Y, et al. The Sonic Hedgehog-Gli pathway regulates dorsal brain growth and tumorigenesis. *Development*. 2001; 128(24):5201–5212.
53. Uziel T, Karginov FV, Xie S, et al. The miR-17∼92 cluster collaborates with the Sonic Hedgehog pathway in medulloblastoma. *Proc Natl Acad Sci USA*. 2009;106(8):2812–2817.
54. Clement V, Sanchez P, de Tribolet N, Radovanovic I, Ruiz i Altaba A. HEDGEHOG-GLI1 signaling regulates human glioma growth, cancer stem cell self-renewal, and tumorigenicity. *Curr Biol*. 2007;17(2): 165–172.
55. Garg N, Po A, Miele E, et al. microRNA-17–92 cluster is a direct Nanog target and controls neural stem cells through Trp53inp1. *EMBO J*. 2013;32(21):2819–2832.
56. Phillips HS, Kharbanda S, Chen R, et al. Molecular subclasses of high-grade glioma predict prognosis, delineate a pattern of disease progression, and resemble stages in neurogenesis. *Cancer Cell*. 2006; 9(3):157–173.
57. Faury D, Nantel A, Dunn SE, et al. Molecular profiling identifies prognostic subgroups of pediatric glioblastoma and shows increased YB-1 expression in tumors. *J Clin Oncol*. 2007;25(10):1196–1208.

58. Schiffman JD, Hodgson JG, VandenBerg SR, et al. Oncogenic BRAF mutation with CDKN2A inactivation is characteristic of a subset of pediatric malignant astrocytomas. *Cancer Res*. 2010;70(2):512–519.
59. Bielen A, Perryman L, Box GM, et al. Enhanced efficacy of IGF1R inhibition in pediatric glioblastoma by combinatorial targeting of PDGFR α/β. *Mol Cancer Ther*. 2011;10(8):1407–1418.
60. Plate KH, Breier G, Weich HA, Mennel HD, Risau W. Vascular endothelial growth factor and glioma angiogenesis: coordinate induction of VEGF receptors, distribution of VEGF protein and possible in vivo regulatory mechanisms. *Int J Cancer*. 1994;59(4):520–529.
61. Goldlust SA, Cavaliere R, Newton HB, et al. Bevacizumab for glioblastoma refractory to vascular endothelial growth factor receptor inhibitors. *J Neurooncol*. 2012;107(2):407–411.
62. Kamal MM, Sathyan P, Singh SK, et al. REST regulates oncogenic properties of glioblastoma stem cells. *Stem Cells*. 2012;30(3):405–414.
63. Schiebe M, Ohneseit P, Hoffmann W, Meyermann R, Rodemann HP, Bamberg M. Analysis of mdm2 and p53 gene alterations in glioblastomas and its correlation with clinical factors. *J Neurooncol*. 2000;49(3):197–203.
64. Becher OJ, Hambardzumyan D, Fomchenko EI, et al. Gli activity correlates with tumor grade in platelet-derived growth factor-induced gliomas. *Cancer Res*. 2008;68(7):2241–2249.
65. Hulleman E, Helin K. Molecular mechanisms in gliomagenesis. *Adv Cancer Res*. 2005;94:1–27.
66. Hong L, Lai M, Chen M, et al. The miR-17–92 cluster of microRNAs confers tumorigenicity by inhibiting oncogene-induced senescence. *Cancer Res*. 2010;70(21):8547–8557.
67. Ernst A, Campos B, Meier J, et al. De-repression of CTGF via the miR-17–92 cluster upon differentiation of human glioblastoma spheroid cultures. *Oncogene*. 2010;29(23):3411–3422.